Efficient Dendrimer–DNA Complexation and Gene Delivery Vector Properties of Nitrogen-Core Poly(Propyl Ether Imine) Dendrimer in Mammalian Cells.

ARTICLE *in* BIOCONJUGATE CHEMISTRY · AUGUST 2013

Impact Factor: 4.51 · DOI: 10.1021/bc400247w · Source: PubMed

Bioconjugate Chemistry

Article

pubs.acs.org/bc

Efficient Dendrimer–DNA Complexation and Gene Delivery Vector Properties of Nitrogen-Core Poly(propyl ether imine) Dendrimer in Mammalian Cells

Abirami Lakshminarayanan,[†] Vijay Kumar Ravi,[‡] Ranjitha Tatineni,[§] Y. B. R. D. Rajesh,[†] Vishal Maingi,[‡] K. S. Vasu,[‡] Nandhitha Madhusudhan,[§] Prabal K. Maiti,*[,‡] A. K. Sood,*[,‡] Saumitra Das,*[,§] and N. Jayaraman*[,†]

[†]Department of Organic Chemistry, [‡]Department of Physics, and [§]Department of Microbiology and Cell Biology, Indian Institute of Science, Bangalore 560 012, India

Supporting Information

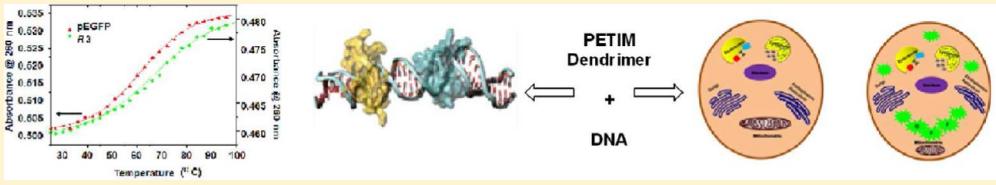

ABSTRACT: Dendrimers as vectors for gene delivery were established, primarily by utilizing few prominent dendrimer types so far. We report herein studies of DNA complexation efficacies and gene delivery vector properties of a nitrogen-core poly(propyl ether imine) (PETIM) dendrimer, constituted with 22 tertiary amine internal branches and 24 primary amines at the periphery. The interaction of the dendrimer with pEGFPDNA was evaluated through UV–vis, circular dichroism (CD) spectral studies, ethidium bromide fluorescence emission quenching, thermal melting, and gel retardation assays, from which most changes to DNA structure during complexation was found to occur at a weight ratio of dendrimer:DNA ∼ 2:1. The zeta potential measurements further confirmed this stoichiometry at electroneutrality. The structure of a DNA oligomer upon dendrimer complexation was simulated through molecular modeling and the simulation showed that the dendrimer enfolded DNA oligomer along both major and minor grooves, without causing DNA deformation, in 1:1 and 2:1 dendrimer-to-DNA complexes. Atomic force microscopy (AFM) studies on dendrimer-pEGFP DNA complex showed an increase in the average *z*-height as a result of dendrimers decorating the DNA, without causing a distortion of the DNA structure. Cytotoxicity studies involving five different mammalian cell lines, using [3-(4,5-dimethylthiazol-2-yl)-2,5-diphenyl-tetrazolium bromide] (MTT) assay, reveal the dendrimer toxicity profile (IC_{50}) values of ∼400–1000 μg mL^{-1}, depending on the cell line tested. Quantitative estimation, using luciferase assay, showed that the gene transfection was at least 100 times higher when compared to poly(ethylene imine) branched polymer, having similar number of cationic sites as the dendrimer. The present study establishes the physicochemical behavior of new nitrogen-core PETIM dendrimer–DNA complexes, their lower toxicities, and efficient gene delivery vector properties.

INTRODUCTION

Dendrimers as newer types of biological vehicles have emerged as a new direction, specifically, in expanding the frontiers of drug and nonviral vector based gene delivery systems development.[1] Rapid endocytosis and nuclease degradations are some of the major hurdles for DNA to cross over cellular barriers before localizing in the cell nucleus and initiating cellular machinery toward protein biosynthesis. Seminal developments to ameliorate degradation of DNA during a gene delivery process include protection methods involving viral and nonviral vectors.[2−6] Cationic poly(amido amine) (PAMAM) dendrimers presenting primary amines at their peripheries were demonstrated early on for their potential as gene delivery systems.[7−11] Issues related to the toxicity and biocompatibility of native, unmodified dendrimers were also addressed. For example, surface modification of PAMAM dendrimers with poly(ethylene glycol) and use of disulfide linkages not only reduced high toxicities, but also increased transfection efficiency by several folds.[12−16] Transfection efficiencies were increased by conjugating the dendrimer with alkyl chains, membrane targeting peptides, arginine–lysine conjugates, and sugars.[17−22] Further, introduction of moieties, such as trimesyl, triethanol, pentaerythritol, and inositol, within the structure demonstrated the importance of dendrimer flexibility on the DNA condensation, toxicities, and *in vitro* transfection properties.[23−26] Hybridization of silica and gold nanoparticles with dendrimers and lysine coated dendrons has promised better transfection and low toxicity.[27−30] Poly(propylene imine) (PPI), carbosilane, phosphorus containing dendrimers, and amphiphilic dendrimers were studied for their

Received: May 17, 2013
Revised: August 1, 2013
Published: August 2, 2013

gene delivery potentials, biodegradability, and serum stabilities.[31] The high toxicities of unfunctionalized dendrimers continue to be a serious impediment, limiting the benefits of dendritic structures, such as monodispersities and uniformly distributed dense peripheries, to develop nonviral vectors. Realizing the requirement of a dendrimer vector which also provides a significantly enhanced range of nontoxicity, we considered a new type of dendrimer platform, namely, a nitrogen-core poly(propyl ether imine) dendrimer.

The nitrogen-core poly(propyl ether imine) dendrimer possesses tertiary amine as the core, as well as the branch point, ether as the linker, and the branch points and linkers are connected through *n*-propyl spacer. A preliminary study on a similar type of dendrimer having a bidirectional oxygen as the core showed gene transfection abilities and toxicity profiles that surpassed those known for other dendrimer types, even when the dendrimer-to-DNA ratio (weight) were in the range of 200−300:1.[32] Encouraged by low toxicity of this dendrimer, an important and significant query as to the reduction in the dendrimer-to-DNA ratio for effective gene delivery was investigated. In this query, it became pertinent and critical to consider the presence of an increased number of cationic sites within a given dendrimer generation, which would increase higher DNA condensation abilities. It was thus considered that construction of a PETIM dendrimer having a three-directional core would afford advantages of a greater number of branching sites and peripheral moieties, and thus more cationic sites, in a lower generation, as opposed to that resulting from a bidirectional core. For example, a third generation oxygen-core dendrimer affords 16 primary amines at the periphery and 10 tertiary amine sites at the interior, whereas the third generation nitrogen-core dendrimer provides 24 primary amine at the periphery and 22 tertiary amine at the interior, even when both dendrimer types possess an identical number of layers between the core and the periphery. With this consideration, we undertook studies of the dendrimer−DNA complexation using the third generation nitrogen-core poly(propyl ether imine) dendrimer. The detailed study required addressing specific queries hitherto unknown on dendrimer−DNA complexation, stoichiometry, nature of interaction, and structural effects on DNA, with the aid of biophysical, physical, and computational techniques. Further, *in vitro* studies were conducted to assess cytotoxicity of the dendrimer and gene transfections of dendrimer−DNA complexes across several cell lines. In the present study, the queries were addressed through (i) physicochemical characterizations by gel retardations, UV−vis, CD spectroscopies, thermal melting measurements, ethidium bromide fluorescence emission quenching, and zeta potential measurements; (ii) molecular dynamics simulations; (iii) atomic force microscopy (AFM) visualizations; (iv) cytotoxicity assays using the dye MTT; (v) qualitative gene transfections using plasmid DNA coding for green fluorescent protein (pEGFP); and (vi) quantitative gene transfections using plasmid DNA coding for luciferase enzyme (pcDLuc), on a number of mammalian cell lines, including hard to transfect cell lines. The studies establish the physicochemical properties, cytotoxicities and gene transfection efficacies of the new nitrogen-core PETIM dendrimer platform.

RESULTS AND DISCUSSION

Synthesis. The third generation nitrogen-core PETIM dendrimer **1** (Figure 1), undertaken in the present study, was synthesized from 24-ester terminated nitrogen-core dendrimer

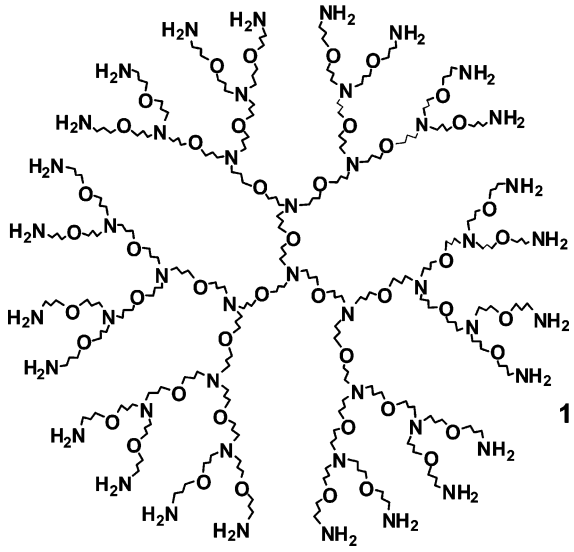

Figure 1. Molecular structure of third generation *N*-core PETIM dendrimer.

(**2**) reported previously (Scheme 1).[33] Thus, reduction of ester moieties in **2** with $LiAlH_4$ and subsequent reaction of the resulting alcohol **3** with acrylonitrile, under base-promoted condition, afforded 24-nitrile terminated dendrimer **4**. Reduction of nitrile in **4**, using Ra−Co catalyst, afforded 24-amine terminated dendrimer **1**. Individual steps of the reaction afforded the product in a good yield. The structural homogeneities of **1**-**4** were confirmed by routine physical methods. Synthesis and structural characterization of **1** are given in the Supporting Information.

Biophysical Characterizations: Gel Retardation Assay. A gel retardation assay on 0.8% agarose gel was conducted in order to verify complexation of the dendrimer with a plasmid DNA, namely, pEGFP. The assay showed a gradient deceleration of the mobility of DNA as the dendrimer-to-DNA weight ratio (*R*) increased progressively (Figure 2). The two bands in the DNA correspond to the supercoiled and open circular forms of plasmid DNA with the supercoiled form showing greater migration owing to its more compact size. A complete complexation was evaluated when DNA was retained fully in the wells that corresponded to *R* values of 0.7−2.5:1. At higher dendrimer-to-DNA ratios from *R* 3 to 5, migration toward cathode was observed with concomitant loss of visibility of the complex, indicating the formation of the complex with net positive charge. A similar observation was reported earlier on the PAMAM dendrimer−DNA complexes.[7] Cathodic migration was evaluated from the migration of the dye front toward cathode for *R* above 3. The inability of ethidium bromide to stain DNA present in the complexes of *R* above 3 suggested that the dendrimer binding led to loss of DNA accessibility. The assay showed qualitatively an effective complexation of dendrimer with DNA, occurring due to electrostatic interaction. Although the weight ratio was considered here, estimation of the corresponding *N*/*P* ratio warranted further studies (*vide infra*).

UV−vis and CD Spectra of Dendrimer−DNA Complexes. The extent with which DNA structure undergoes changes as a result of interaction with dendrimer was investigated through UV−vis and CD spectral studies. The changes in the intensity of absorbance at λ_{260} of the DNA provide a clue to its sensitivity upon interaction with the

dx.doi.org/10.1021/bc400247w | *Bioconjugate Chem.* 2013, 24, 1612−1623

Scheme 1

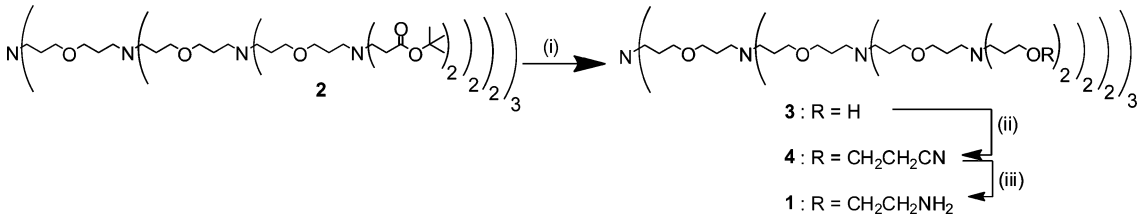

Reagents and conditions: (i) LAH, THF, 0 °C to rt, 4 h; (ii) $H_2C{=}CH\text{-}CN$, aq. NaOH, 63 h, rt; (iii) Ra-Co, H_2, H_2O, 70 °C, 40 bar.

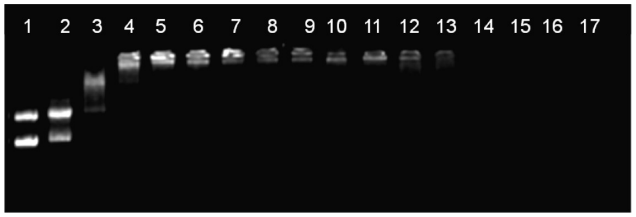

Figure 2. Gel retardation assay of dendrimer-pEGFP complexes. Samples (20 μL) of dendrimer-pEGFP were prepared by incubating 2 μg of DNA along with the required amounts of dendrimer in PBS (pH7.4) for 20 min. The complexes were electrophoresed through 0.8% agarose gel using Tris acetate-EDTA buffer system (pH 8). The DNA was visualized by ethidium bromide staining. Lanes 1: pEGFP alone; 2: R = 0.1; 3: R = 0.3; 4: R = 0.5; 5: R = 0.7; 6: R = 0.9; 7: R = 1.1; 8: R = 1.3; 9: R = 1.5; 10: R = 1.7; 11 R = 1.9; 12: R = 2.1; 13: R = 2.5; 14: R = 3; 15: R = 4; 16: R = 5; and 17: dendrimer alone.

dendrimer. For this purpose, pEGFP DNA (10 μg mL^{-1}) in PBS buffer (pH 7.4) was titrated, using a stock solution of dendrimer (20 mg mL^{-1}) in the same buffer. The titration was performed according to dendrimer–DNA weight ratio (R) and the spectrum was recorded after equilibration for 20 min. A reduction in the intensity was observed as R increased to 3:1 from that of DNA solution alone (Figure 3a), which indicated a rigidity of the DNA structure[34] upon complexation with dendrimer. However, at higher ratios, an increase in the intensity was seen, indicating a reduction in the double strand stability of the DNA.

A thermal melting measurement of the DNA double strand denaturation–renaturation was undertaken so as to assess the observations of UV–vis spectra of dendrimer–DNA complexes. DNA double strand undergoes unwinding when heated, and at a temperature called thermal melting (T_m), the double strand unwinds to a single strand and the process is monitored by sharp increase in the absorption (λ_{260}). On cooling, a re-registering to the double strand occurs. An increase in the stability in the double strand is marked by the higher T_m, whereas reduction in the stability of the double strand lowers the T_m. With this sensitive method available to assess the stability, the thermal melting experiments of dendrimer–pEGFDNA complexes were undertaken. The study was conducted in three ratios (weight), namely, 1:1, 3:1, and 5:1 dendrimer-to-DNA and compared with T_m of DNA alone. The measurements were conducted using preformed pEGFP DNA (10 μg)-dendrimer (0, 10, 30, and 50 μg) complexes, in PBS buffer (pH 7.4) and at a rate of heating 3 °C min^{-1}. T_m of DNA alone, measured as the midpoint of 25–75% raise in the sigmoidal curve, was identified to be 62.5 °C. Upon 1:1 and 3:1 complexation of dendrimer with DNA, the T_m was found to increase to 67 and 67.5 °C (Figure 3b), respectively, clearly denoting the ensuing stability, by 5–5.5 °C, of the double strand in the complex. However, the double strand unwinding became facile and the T_m was found to be 61.5 °C for the 5:1 complex. These observations conform with UV–vis spectral studies, wherein the 5:1 complex showed nearly equal optical density at 260 nm as that of the DNA alone, whereas the lower ratios showed a hypochromism (Figure 3a). Considering that

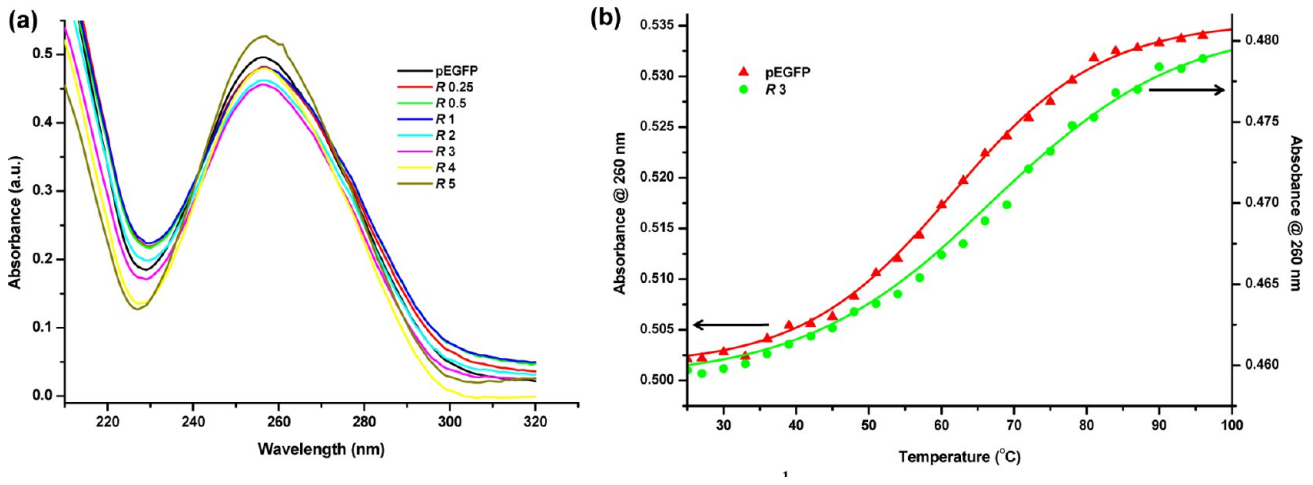

Figure 3. (a) UV–vis spectral profile of pEGFP (10 μg mL^{-1}) and pEGFP-dendrimer complexes in PBS (pH = 7.4) at various weight ratios (R) of dendrimer:DNA. Complexes were equilibrated for 20 min prior to recording the absorbance. (b) T_m profile of pEGFP (10 μg mL^{-1}) and dendrimer–pEGFP complexes at R of 3, corresponding to 30 μg of dendrimer. The complexes were prepared in PBS (pH = 7.4), equilibrated for 20 min, and heated at a rate of 3 °C min^{-1}.

dx.doi.org/10.1021/bc400247w | Bioconjugate Chem. 2013, 24, 1612–1623

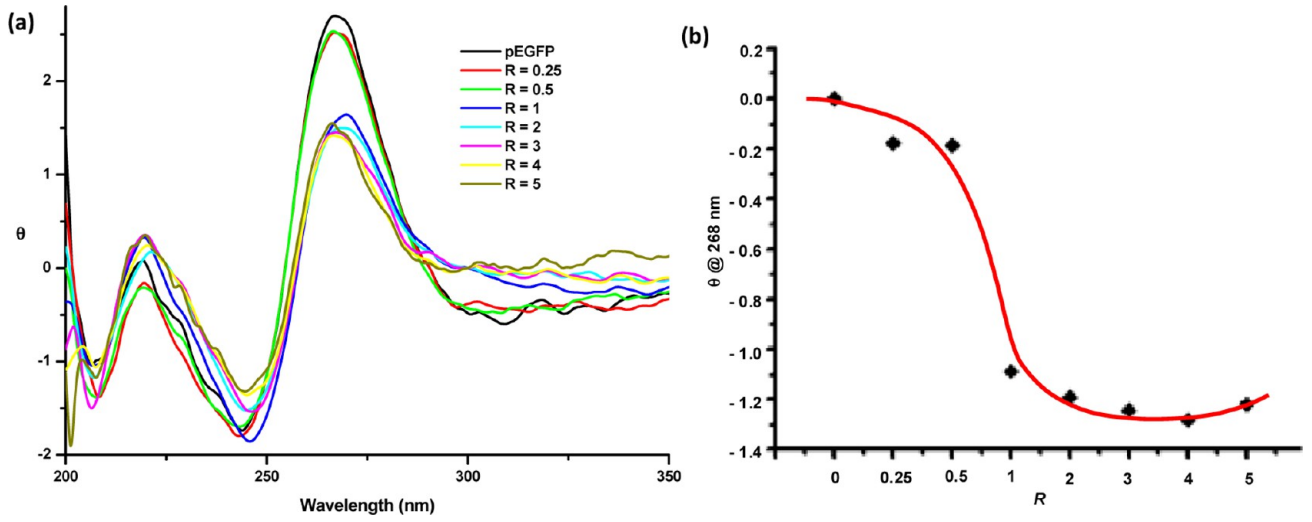

Figure 4. CD profile of (a) pEGFP upon titration with dendrimer at various weight ratios (R): 0, 0.25, 1, 2, 3, 4, and 5 in PBS (pH = 7.4); concentration of DNA used is 50 μg mL^{-1}, T = 298 K. The molar ellipticity (θ) is expressed in units deg M^{-1} cm^{-1}; (b) a plot of R *vs* change in ellipticity ($\Delta\theta$) at 268 nm.

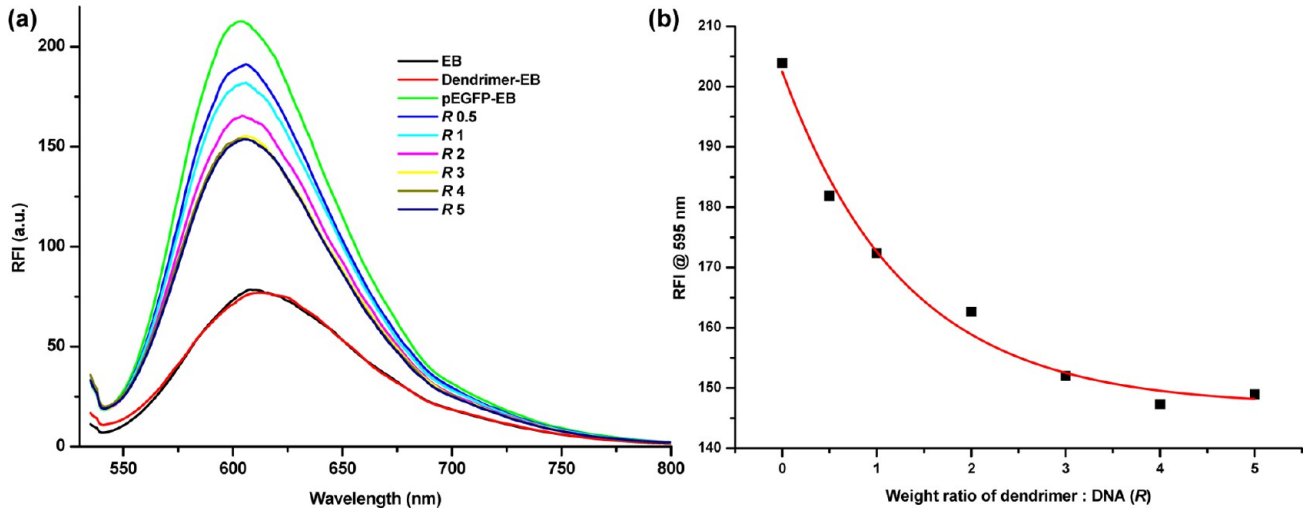

Figure 5. (a) Fluorescence emission spectrum of ethidium bromide (EB) in the presence of dendrimer−pEGFP complexes at different weight ratios (R): 0, 0.5, 1, 2, 3, 4, and 5 in PBS (pH = 7.4). DNA:EB ratio is 6:1 and DNA concentration used is 10 μg mL^{-1}. The emission intensity of EB alone in PBS as well as in the presence of dendrimer alone (150 μg mL^{-1}) is also indicated. (b) A plot of the relative fluorescence intensity (RFI) of the EB-pEGFP-dendrimer complexes at various R values.

ratios above 3:1 lead to a net positive charge of the complex (*vide infra*), the T_m results show that the net positive charge of the complex might hamper the DNA stability. In the cooling cycle in each of the above ratios, a nearly complete re-registering of the double strand was observed, thereby implying that the complexation did not severely affect the DNA constitution and the interaction is electrostatic in nature. The only comparison for the thermal melting of dendrimer−DNA complex is seen with PAMAM dendrimer−DNA complexes, wherein a moderate increase by ∼3−8 °C was observed, depending on the dendrimer generation, with peripheral amine groups of either 16 or 256.[35]

In order to verify changes to DNA conformation upon interaction with dendrimer, CD studies were performed. CD titrations were conducted with DNA (50 μg mL^{-1}) in PBS buffer (pH 7.4), using a stock solution of dendrimer (20 mg mL^{-1}) in the same buffer, and the titration was conducted according to dendrimer-to-DNA weight ratio and measured after the equilibration period. The DNA showed two positive Cotton bands at 268 and 219 nm, and two negative Cotton bands at 243 and 207 nm. Upon addition of the dendrimer, the band at 268 nm underwent a larger change in the intensity, when compared to the other three bands (Figure 4). A plot of R *vs* change in ellipticity at 268 nm showed that most change occurred when R value was between 0.5 and ∼2. In conjunction with the observation in UV−vis spectra, these CD spectral intensity changes indicate a DNA structure becoming more rigid, as compared to DNA alone, although the spectral intensity appeared to increase slightly at the ratio R of 5.

Ethidium Bromide Emission Quenching Assay. Continuing assessment of the DNA structure in the dendrimer−DNA complex, ethidium bromide emission quenching assay was examined. The dye ethidium bromide stacks in between the base pairs, which enhances the emission intensity of the dye, when compared to the dye alone in the bulk solution. A change in the DNA structure would affect the stacking interaction and

dx.doi.org/10.1021/bc400247w | *Bioconjugate Chem.* 2013, 24, 1612−1623

(a)

	Zeta potential (mV)	Electrophoretic mobility (V/cm)
DNA	-23.87	-1.244
R 0.25	-21.72	-1.142
R 0.5	-13.35	-0.698
R 1	-6.76	-0.352
R 2	9.47	0.494
R 3	10.22	0.504
R 4	16.85	0.876
R 5	21.65	1.127
Dendrimer	28.35	1.476

(b)

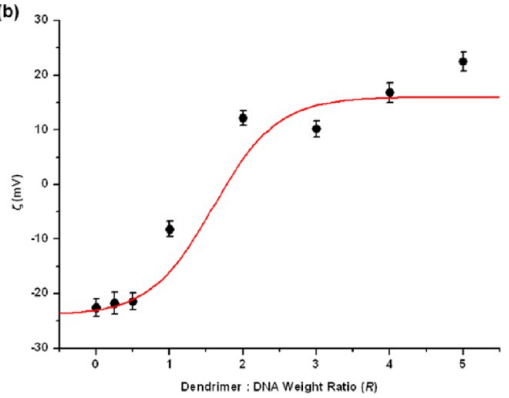

Figure 6. (a) Table of the zeta potential (ζ) and electrophoretic mobility (μ) values at various *R* ratios. (b) Zeta potential measurements of pEGFP and pEGFP-dendrimer at various weight ratio (*R*) in HEPES buffer (pH −7.4) at 25 °C: *R* 0.25, 0.5, *R* 1, *R* 2, *R*3, *R* 4, *R* 5.

thus the resulting emission intensity of the dye. A pre-equilibrated complex of ethidium bromide-pEGFP DNA (1:6 mol ratio) in PBS was titrated with a solution of the dendrimer in PBS buffer (pH 7.4) (Figure 5). The concentration of DNA was 30 μg mL^{-1}, whereas that of the dendrimer stock solution was 25 mg mL^{-1}. A gradual reduction in the emission intensity was observed as *R* increased until ∼3, beyond which the increasing ratio affected change in the emission intensity only marginally. The reduction in the emission intensity pertained to a change in the DNA structure, and as evaluated by UV−vis and CD spectral measurements, the DNA structure became more compact upon binding with dendrimer, especially at lower *R* values.

Zeta Potential Measurements. In order to verify the charge neutralization in dendrimer−DNA complexes, zeta potential measurements were carried out on pEGFP and their complexes with the dendrimer. An aq. solution of DNA (10 μg mL^{-1}) in HEPES buffer (pH 7.4) has a zeta potential of −23.8 mV, whereas aq. dendrimer solution (50 μg mL^{-1}) in the same buffer exhibited a zeta potential of +28.3 mV. When DNA was titrated with dendrimer, the negative value gradually reduced and eventually reached the positive zeta potential values.

The values of electrophoretic mobility (μ) and the corresponding zeta potential values for pEGFP, dendrimer, and their complexes different *R* values are indicated in Figure 6a. Zeta potential is calculated from the electrophoretic mobility measurements using eq 1.[36]

$$\zeta = \frac{3\eta}{2\varepsilon_0\varepsilon_r f(\kappa_D a)}\mu \qquad (1)$$

where η is the viscosity of water; ε is the vacuum (ε_0) and relative permittivity (ε_r); $f(\kappa_D a)$ is the Henry function, where κ_D is reciprocal Debye length and *a* is the particle radius. Figure 6b shows a plot of zeta potential *vs* *R* values, from which electroneutrality was measured at dendrimer-to-DNA ratio (weight) of 1.8:1. At *R* values above 2, the zeta potential remained positive, denoting cationic charges predominating in the solution. Further, these zeta potential values demonstrated a strong electrostatic interaction between DNA and the dendrimer. The electroneutrality at ratio *R* 1.8:1 is in good agreement with that observed by spectroscopic studies and ethidium bromide emission quenching assay (*vide supra*).

Molecular Dynamics Simulations. The series of experiments above showed that the DNA structure became more compact upon complexation with dendrimer and the zeta potential measurement showed that the electroneutrality occurred at a dendrimer-to-DNA weight ratio of 1.8:1. The structural behavior of the DNA−dendrimer complexes was investigated further at a microscopic level through molecular dynamics (MD) simulations. Three possibilities of dendrimer−DNA complexations were studied, each with one DNA strand and 1 to 3 dendrimer molecules. Recent experiments suggest strong dendrimer−DNA interactions occurring at both the major and minor grooves.[10] Based on these experimental observations, dendrimers were placed in either the major groove or minor groove of DNA as the initial condition. Long time scale atomistic MD simulation was performed using AMBER11 package.[37] Instantaneous snapshots of the dendrimer−DNA complexes at a few nanosecond time intervals are shown in Figures 7−10.

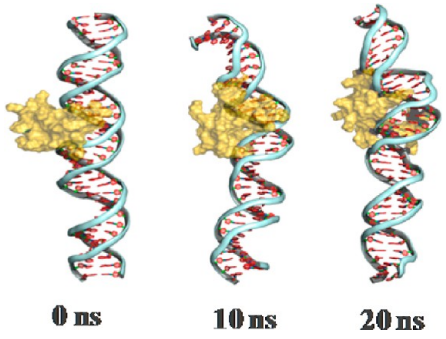

Figure 7. Instantaneous snapshots of system showing complex formation between one DNA strand and one dendrimer molecule. The dendrimer was placed in the major groove. This system shows wrapping of the PETIM dendrimer around DNA.

Simulation studies for the 1:1 and 2:1 complex (Figures 7 and 8) showed that dendrimer enfolded the DNA without causing DNA deformations. This is in contrast to the DNA enfolding the dendrimer as in the case of PAMAM dendrimers.[10] In the case of single PAMAM dendrimer binding to DNA, significant bending of the DNA double helix was observed. The simulations reveal that dendrimer placed in both the major and minor grooves of DNA retain a stable configuration and maintain a stable interdendrimer distance.

To validate the simulation studies and the stability of one DNA and two dendrimers system (Figure 8), the center of mass distance (COM) between the two dendrimers over 40 ns long run was calculated (Figure 11). After 20 ns, COMs distance was almost stable and fluctuated between 43 and 45 Å.

dx.doi.org/10.1021/bc400247w | *Bioconjugate Chem.* 2013, 24, 1612−1623

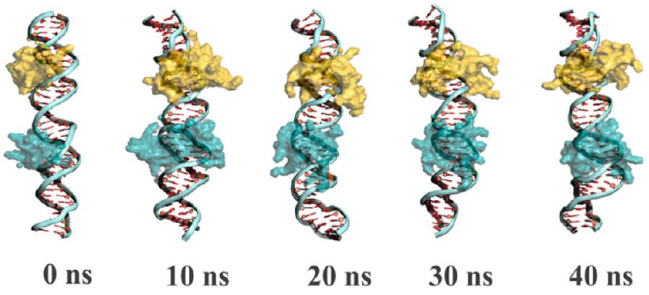

Figure 8. Instantaneous snapshots of system showing complex formation between one DNA strand and two dendrimer molecules. The dendrimers were positioned on adjacent major grooves. This system again showed wrapping of the PETIM dendrimer around DNA. An enlarged snapshot is shown in Figure 9.

Figure 9. Enlarged 40 ns snapshot of DNA-two PETIM dendrimer (golden and cyan-colored) can be seen enfolding major grooves of DNA.

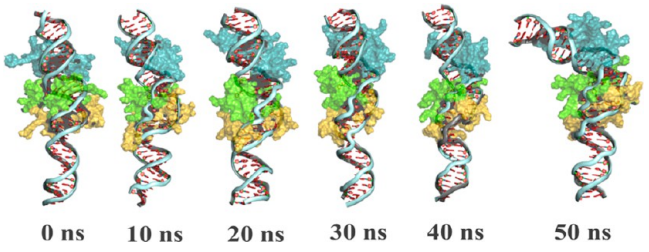

Figure 10. Instantaneous snapshots of the complex formation between one DNA strand and three dendrimer molecules. The dendrimers were positioned on two adjacent major grooves and the third molecule on the opposite major groove. Base pair destruction resulting in DNA bending can be visualized in 50 ns snapshot.

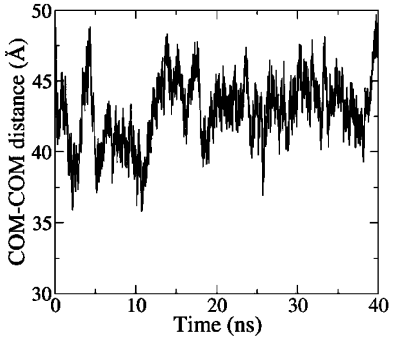

Figure 11. COM distance between two PETIM dendrimers in the case of 2:1 complex over 40 ns long MD simulation. The COM distance is found to be stable between 43 and 45 Å.

Complexes with 3:1 stoichiometry was also studied by placing two dendrimers at adjacent major grooves and positioning the third at the major groove between them on the opposite side. However, the DNA base pair destruction started appearing for this system (Figure 10). In conjunction with spectroscopic studies, the results of simulation showed that the compactness of DNA structure might be hindered at higher *R* values.

Further, MD simulations also revealed that a dendrimer molecule enfolded nearly one helical twist of the DNA double strand, which would entail only ∼one-fourth of 46 cationic sites on the dendrimer molecule to be under electrostatic interaction with the DNA. In light of this, the *N*/*P* ratios are likely to be considerably lower than that arising due to participation of all the available cationic sites on the dendrimer.

AFM Visualization of Dendrimer−DNA Complex. Physical evaluation of the dendrimer−DNA complex was undertaken using AFM method. PAMAM dendrimer−DNA complexes were shown previously to be condensed resulting in spherical or globular particles.[38,39] Contraction of precoated DNA upon addition of dendrimer and other structural features, such as multiple crossovers, dense interior structures, and corona or disc-like complexes, were visualized for differently modified PAMAM dendrimer−DNA complexes.[35,39−41] In the present study, third generation nitrogen core PETIM dendrimer (0.1 ng mL^{-1}) and dendrimer−plasmid DNA complexes (*R* = 1:1 and 5:1) were used and distinct conformational changes were observed in the DNA. The morphology of PETIM dendrimer (Figure 12A) has height distribution spanning from 0.23 to 0.75 nm (Figure 12E). The plasmid DNA, pcDNA Luc, was visualized in the presence of Mg^{2+} ions on negatively charged Muscovite mica. The DNA showed a closed circular structure with about three nodes and depicted supercoiled and wreath-like structures (Figure 12B). The average *z*-height of pcDNA Luc was measured to be 0.51 nm with a standard deviation of ±0.13 nm (marked with a red line in the figure). The morphology of the pcDLuc upon complexation with the dendrimer was visualized without the Mg^{2+} ions. The 1:1 complex was visualized as a DNA strand being decorated by dendrimers with a *z*-height of 1.5 ± 0.75 nm (Figure 12C). Ritort and co-workers have shown a similar type of decoration of PAMAM dendrimer on λ-phage linear DNA.[42] We note that DNA in the presence of dendrimer (*R* = 1:1) is an open strand of uncondensed form, similar to the uncondensed form in the presence of a linear methacrylate based polycationic polymer (PDMAEMA).[38] This is different from the condensation of plasmid DNA in the presence of PAMAM based dendrimers[43,44] As expected for the *R* = 5:1 complex, the DNA is more decorated with dendrimer with an average *z*-height of 4.5 ± 1.5 nm (Figure 12D). Importantly, there is no global deformation of the DNA upon complexation with dendrimer on the mica surface and the arrangement of dendrimer along the DNA backbone is in agreement with the results of the molecular dynamics simulations and UV−vis and CD spectroscopic studies (*vide supra*).

Evaluation of Cytotoxicity and Gene Transfection. Verification of cytotoxicity of the dendrimer was undertaken prior to gene transfection studies of the dendrimer−DNA complexes. The toxicity of the dendrimer was evaluated using MTT assay on five different mammalian cell lines, namely, kidney derived cells BHK21, liver derived cells Huh7, cervical cancer cells HeLa S3, neuro glial cells CHME3, and lung carcinoma cells A549. Figure 13 shows the toxicity profile of dendrimer on the above cell lines after 48 h, wherein the concentration at which 50% of the cells survive (IC_{50}) was

dx.doi.org/10.1021/bc400247w | *Bioconjugate Chem.* 2013, 24, 1612−1623

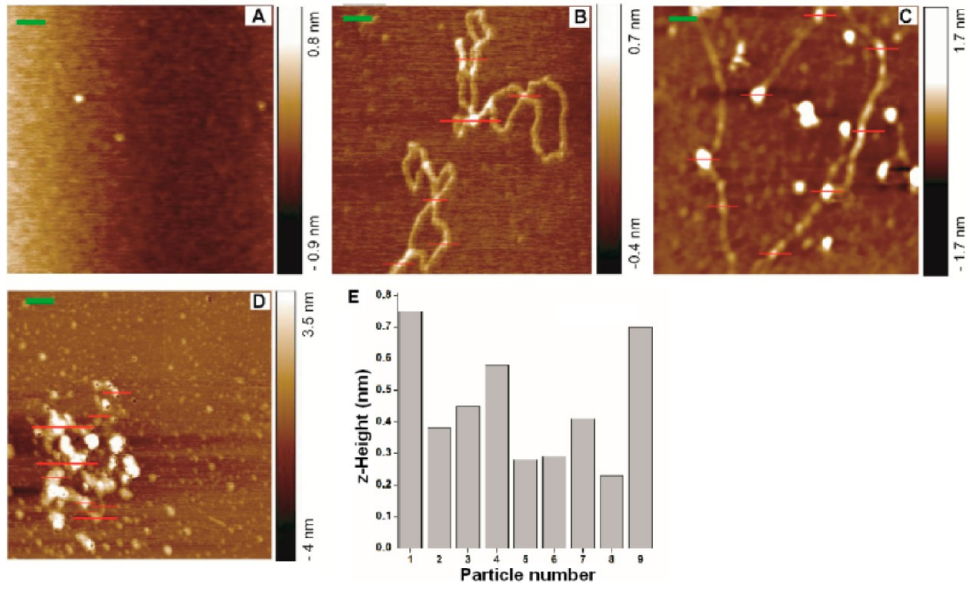

Figure 12. Tapping mode AFM images of dendrimer, DNA, and dendrimer–DNA complex. (A) 0.1 ng mL^{-1}dendrimer; (B) 0.1 ng mL^{-1}pcDNALuc; (C) R = 1:1 complex showing decorated dendrimers dispersed inhomogeneously along with the DNA strand; (D) R = 5:1 complex showing dendrimer embedded to DNA strand. (E) z-height distribution of dendrimer. Scale bar = 100 nm.

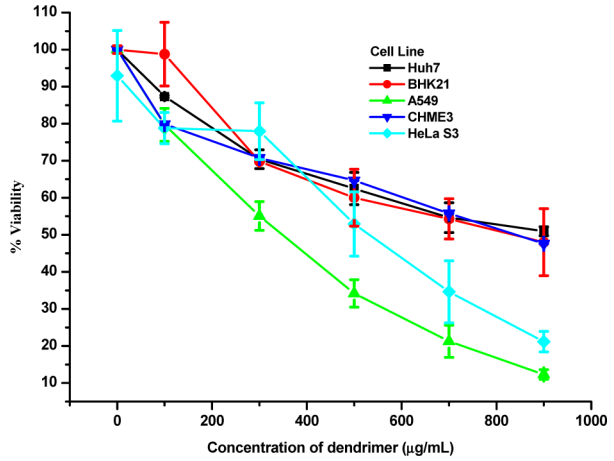

Figure 13. Toxicity profile of PETIM dendrimer, assessed by MTT assay after 48 h in five different mammalian cell lines.

found to be in the range of 400–900 μg mL^{-1}, depending on the cell type.

These IC_{50} values are high when compared to other types of dendrimers for which the IC_{50} values are known, as shown in Table 1. Although the cell types on which the assays were performed differ, in comparison to other dendrimer types known, it is clear that the cytotoxicity of the dendrimer studied herein exhibits more than 1 order of magnitude lower toxicity. The PETIM dendrimer having the bidirectional oxygen core showed a similar IC_{50} value with BHK21 cells used to assess the toxicity.[32] The presence of ether moieties in the PETIM dendrimer series might account for the otherwise extremely reduced IC_{50} values seen generally with the tertiary amine branched and primary amine terminated dendrimers.

Gene Transfection. A qualitative gene transfection study was undertaken initially using plasmid DNA coding for green fluorescent protein (pEGFP) in order to test the potential of the dendrimer to deliver DNA into cells. The cell membrane being negatively charged, a PETIM-plasmid DNA complex with

Table 1. Compilation of IC_{50} Values of Different Types of Dendrimers and PEI Polymer in Various Cell Lines[c]

	MW (gmol^{-1})	IC_{50} (μg mL^{-1})	cell lines tested
Poly(amido amine) (PAMAM)[45,46]	6909	50–400	B16F10, HepG2, CCRF, HaCat, SW480
Poly(propylene imine) (PPI)[45,46]	3508	5–50	B16F10, HepG2, CCRF, HaCat, SW480
Poly(ether imine) (PETIM)[32, this work]	5200	400–1000	Huh7, BHK21, A549, HeLa S3, CHME3
	7043	>1000	
Carbosilane dendrimer[47]	4598	25	PMBC
	3008	>20[b]	
Phosphorus containing dendrimer[48,49]	16280	25	N2a[a], HeLa, HUVEC, HEK 293
	33702	100	
Poly(ethylene imine) polymer[50–52, this work]	2000	>1000	BHK21, COS7, HEK293,A431
	25000	20–40	

[a]IC_{50} values calculated at 24 h. [b]IC_{90} value calculated at 36 h is ~20 μg mL^{-1}. [c]The values are after ~48 h unless indicated.

net positive charge would facilitate the easy passage of the complex into the cell and prompt gene delivery. The ability of PETIM dendrimer to deliver plasmid DNA was optimized first by transfecting various ratios of dendrimer–pEGFP complexes in cultured cells and imaging the green fluorescence protein (GFP) expression. A ratio R of 5:1 was found to exhibit optimum gene transfection, which, at the outset, is much lower than the ratio R of 26:1 used in the case of oxygen-core PETIM dendrimer.[32] This observation corroborates the fact that a nitrogen initiator core affords dense charges at a lower dendrimer generation. As seen from the zeta potential measurements, the complex at R of 5:1 is positively charged (+21.2 mV) and thus correlates to the high transfection efficiency. The dendrimer concentration used in transfection studies was less than 50 μg mL^{-1}, at which concentration, it is completely non-cytotoxic. The GFP expression resulting from use of different types of mammalian cell lines, after 48 h, is shown in Figure 14. Across the cell lines, the GFP expression

dx.doi.org/10.1021/bc400247w | Bioconjugate Chem. 2013, 24, 1612–1623

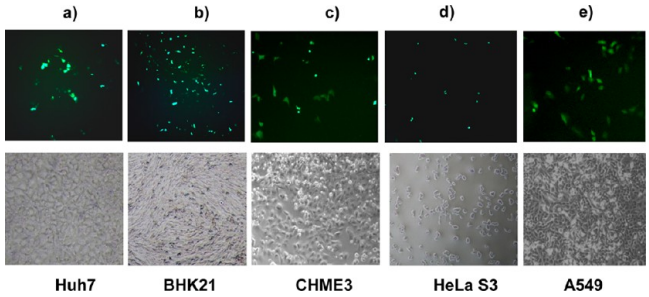

Figure 14. Fluoroescence and bright images (magnification = 20×) for the GFP transfection across different mammalian cell lines: (a) Huh7, (b) BHK21, (c) CHME3, (d) HeLa S3, and (e) A549 after 48 h. Dendrimer−pEGFP complexes at *R*5 were transfection after an equilibration of 20 min in Opti-MEM. The transfection expression was conducted using 10^5 cultured cells in each case.

varied indicating that the delivery efficiency of dendimer in the cell lines was different. The corresponding bright field images indicate that the cells are healthy and intact. Further, the dendrimer−DNA complexes were equilibrated for time from 20 to 60 min in order to test if longer duration of complexation would increase the transfection efficacy; however, only marginal or no effect on the extent of transfection was observed.

The use of *R* higher than 5:1 dendrimer-to-DNA led to a decrease in the GFP expression. Although it is difficult to ascertain, we surmise that the release of dendrimer−DNA complex is affected in order to be accessible by transcription factors. Previous studies by Baker and co-workers showed that *in vitro* transcription is inhibited when large amounts of PAMAM dendrimer are used to complex luciferase expressing gene.[53] It is likely that a high electrostatic interaction in the presence of large amounts of dendrimer would restrain the dynamic complexation phenomenon, and thus make the DNA inaccessible to transcription factors.

Use of lysomotropic agents, such as chloroquine, DEAE dextran, and glycerol, is known to increase the transfection efficiencies, since endosomal internalization is postulated as a rate limiting step in transfection.[7] Accordingly, experiments were conducted in the presence of chloroquine (25−100 μM), and it was found that the transfection efficiency was not affected considerably (Figure 15). We presume that amine

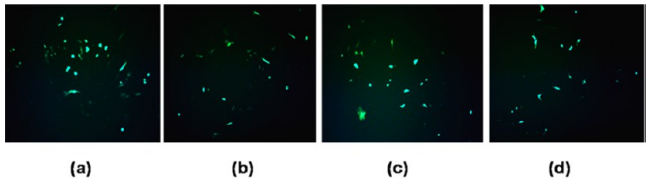

Figure 15. Transfection in BHK21 cells in the presence of varying concentrations of chloroquine, after 48 h: (a) no chloroquine; (b) 25 μM; (c) 50 μM; and (d) 100 μM. The transfection experiment was conducted using 10^5 cultured cells in each case. Complexes were prepared in serum free medium and transfected in medium containing the indicated concentration of chloroquine.

moieties constituting the dendrimer are sufficient to participate in effective lysosomal osmosis, so as to aid the delivery of DNA into cells via endolysosomal escape. Similar observations were reported for the PAMAM dendrimers with trimesyl core[19] as well as for different generations of dendrimers.[8]

Further, gene transfections were also conducted in the presence of serum, in order to verify the effect of serum on the stability of the complex, and the resulting transfection efficiency. Serum trasfections are important from the point of view of mimicking an in vivo system delivery. pEGFP−PETIM dendimer complexes at *R* 5:1 were tested for their transfection ability in BHK21 cell line in the presence of 10% serum. The extent of transfection appeared to be reduced in comparison to transfection in the absence of serum (Figure 16).

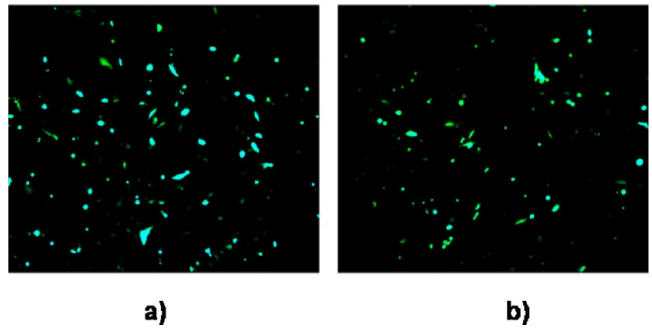

Figure 16. Effect of the presence of serum on the transfection of dendrimer−pEGFP complexes in BHK21 cells: (a) Transfections carried out in the absence of serum; (b) transfection carried out in the presence of 10% serum. The transfection experiment was conducted using 10^5 cultured cells in each case and the cells were imaged for GFP expression after 48 h form the time of addition of complexes.

Serum proteins are known to interfere with the uptake of DNA−vector complexes and also interact with the positively charged complexes leading to aggregate formation which is rapidly cleared, thus resulting in a decrease in transfection efficiency.[54] The stability of DNA−dendrimer complexes is also known to decrease in the presence of serum, again affecting the gene delivery capacity of dendrimers.[19,23]

Upon identifying effective gene transfection through qualitative GFP expression, quantification of the expression efficiency was conducted through transfection of pcDNA Luc, followed by an enzymatic assay measuring the luciferase activity. Thus, luciferase as a reporter gene was used to quantify the expression levels of gene in the cell. In the assay, polyethylene imine (PEI, mw 2000 g mol^{-1}) was used as a control, as PEI is used widely not only for transfections,[55] but also for the number of cationic sites in PEI that matched closely the dendrimer studied herein. The dendrimer possessed 46 cationic sites, whereas the PEI polymer presented on an average 44 cationic sites. Since the optimized ratio *R* for effective gene delivery was 5:1, the same ratio of dendrimer:luciferase gene was used to transfect the cell lines.

We have used a wide choice of mammalian cell lines in our study, namely, the liver derived Huh7 (hepatocellular carcinoma) cells, cells of kidney origin (BHK21, Baby hamster kidney), microglial cells, CHME3, HeLa S3 (cervical cancer) cells, and lung derived A549 (lung carcinoma) cells to study and the levels of transfection in cells offering different challenges for transfection. BHK21 cells are robust cells, widely used for transfection experiments, and are known to be compatible for transfcetions. A549 cells are generally hard to transfect owing to a additional mucous membrane over the cell membrane. Moderately trasfectable CHME3 cells and spinner culture adapted HeLa S3 cells were also used to test the transfection capabaility of dendrimers. Huh7 cells, derived from

dx.doi.org/10.1021/bc400247w | *Bioconjugate Chem.* 2013, 24, 1612−1623

the liver, can harbor the HCV (human hepatocellular carcinoma virus) and effective transfection in these cells would open a new platform for delivery of drugs and antisense oligomers to combat HCV infection.

The ratio *R* 5 was used to quantitate the levels of luciferase protein expression at varying time intervals in the cell lines described above. The luminescence obtained upon cleavage of substrate by the enzyme was measured and normalized with the amount of protein. The studies showed that the gene expression levels increased with time thereby indicating the successful delivery and processing of the plasmid DNA (Figure 17). Considering the short half-life of luciferase enzyme, the

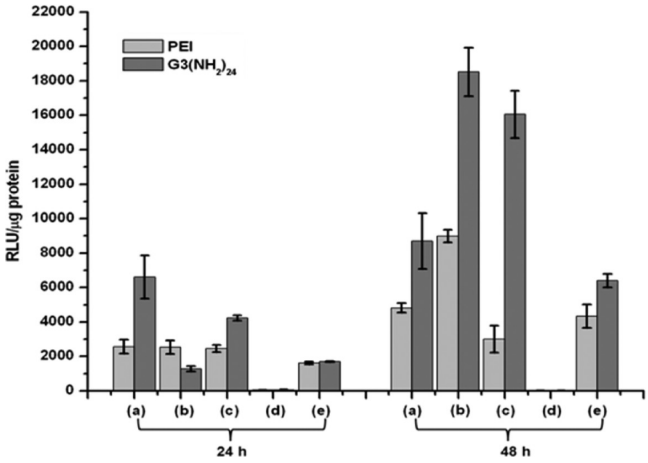

Figure 17. Luciferase assay on various cell lines (a) Huh7; (b) BHK21; (c) CHME3; (d) HeLa S3; (e) A549, at 24 and 48 h. Transfection experiments were carried out on 10^5 cultured cells in each case at the optimized ratio *R* 5:1. The cell lysate was assayed for luciferase enzyme activity and the readings were normalized to the amount of protein.

results suggested slow and sustained release of the luciferase DNA from the dendrimer complex. HeLa S3 cells showed poor transfection with both the dendrimer as well as PEI possibly because the spinner culture adapted cells were grown as monolayers and used for transfection studies. Further, it was observed that the transfection efficiencies of the luciferase gene by the dendrimer and PEI vectors were significantly different; the dendrimer vector exhibited at least 100 times better transfection efficiency with CHME3 cells, 80 times better in BHK21 cells, and 50 times better with Huh7 cells than the PEI polymer on these cell lines, thereby reflecting enormous advantage of the dendrimer structure when compared to a polymer structure, even when the number of cationic sites are similar. From the biophysical studies we postulate that the dendrimer−DNA weight ratio (*R*) 5:1 helps improve decomplexation of DNA once inside the cells thus resulting in higher levels of gene expression.

CONCLUSION

The present study establishes the complex formation and structural rigidity of plasmid DNA upon interaction with PETIM dendrimer, as studied through UV−vis, CD spectroscopies, thermal melting, and ethidium bromide fluorescence quenching techniques. The zeta potential studies indicate the formation of a positively charged complex which can mediate gene transfections efficiently. The microscopic picture of the dendrimer−DNA complex was assessed through molecular dynamics simulations that showed dendrimer to be in the major or minor groove of the DNA giving rise to bead-on-string like structure. Importantly, the dendrimer enfolded the DNA without bending of DNA. This was further confirmed by CD studies which showed that the overall B-DNA structure of plasmid DNA is retained upon binding with PETIM dendrimer. Observations of simulations were ascertained further through AFM studies, wherein the dendrimer was found to coat the DNA along its length. The nitrogen-core PETIM dendrimer undertaken for the present study was seen to exhibit toxicity profiles (IC_{50}) in the range of ~400−900 μg mL^{-1}, depending on the cell line. Gene transfection efficiency was assessed by the GFP expression method, which was augmented further by a luciferase assay so as to quantitate the gene transfection. In comparison to poly(ethylene imine) polymer, the dendrimer exhibited 50 to 100 times better transfection efficiency, depending on the cell line used. Having identified the DNA binding and gene delivery properties of PETIM dendrimer, further work will focus on PETIM dendrimers functionalized with cell-specific ligands, such as sugars and peptides, so as to achieve target specific gene delivery.

EXPERIMENTAL METHODS

UV−vis and CD studies. UV−vis absorption spectra were recorded on Perkin-Elmer Lambda 35 spectrophotometer. pEGFPDNA (10 μg mL^{-1}) in phosphate buffer saline (PBS) (pH 7.4) was titrated with a solution of dendrimer in PBS buffer (stock solution: 20 mg mL^{-1}). The UV−vis spectrum was recorded after 20 min of equilibration of the complex, after each addition. Titration was performed up to a dendrimer−DNA ratio (*R*) of 5. For thermal melting experiments, complexes at *R* 1, 3, and 5 were prepared in the manner described above in PBS. The rate of heating was controlled with the help of PTP-1 Peltier system at 3 °C min^{-1} and the absorbance was recorded from 25 to 96 °C. A similar protocol was followed to record the CD spectra of dendrimer−DNA complexes. A solution of plasmid DNA (50 μg mL^{-1}) was titrated with a dendrimer solution (stock solution 20 mg mL^{-1} in PBS), equilibrated for 20 min, and the CD spectrum was recorded on a Jasco J815 dichrograph at a scan rate of 240 nm min^{-1} in a 2 mm quartz cuvette. The scans were processed by subtracting the blank reading and smoothing with a Savitsky-Golay function (5 points). Titration was performed to dendrimer−DNA ratio (*R*) of 5.

Ethidium Bromide Emission Quenching Assay. Fluorescence emission spectra of ethidium bromide (EB) were recorded on Varian Carey Eclipse Fluorimeter. A 10 mm stoppered rectangular silica cell was used for recording the fluorescence at a constant temperature of 25 °C. A solution of plasmid DNA (30 μg/mL) in PBS (pH = 7.4) was incubated for 10 min with EB at a molar ratio of 6:1 DNA:EB and the fluorescence spectrum was recorded by exciting at 520 nm and recording the emission in the 535−800 nm region. The solution was then titrated with dendrimer (5 mg/mL) in PBS (pH = 7.4). After equilibration for 20 min following each dendrimer addition, the fluorescence spectrum was recorded. The emission and excitation band slits were fixed at 10 nm for all the recordings. Fluorescence of EB in PBS (pH = 7.4) and EB-dendrimer (150 μg/mL) in PBS (pH = 7.4) were also recorded. The concentration of EB (1.6 μM) was kept constant in all cases.

Computational Approaches and Simulation Methodology. Initial coordinates for amine terminated nitrogen core

generation 3 PETIM dendrimer were generated with our in-house Dendrimer Builder Toolkit[56,60] which uses various AMBER modules for polymer building. The methodology used to simulate the DNA-dendrimer system was similar to our earlier[10,66] works and is described briefly below.

In our (MD) simulation B-DNA was used (GCCGCGAGGTGTCAGGGATTGCAGCCAGCATCTCGTCG), which was studied earlier[57,58] with AMBER03 force field.[59] General Amber Force Field (GAFF) was used for dendrimer.[61] We have considered three cases: DNA complex with single PETIM, DNA complex with two PETIM dendrimers, and DNA complex with three PETIM dendrimers.

With the help of LEAP module in AMBER, dendrimer(s) was (were) placed in the major groove(s) of dsDNA taking care and avoiding any atomic overlaps. In the case of DNA−two dendrimer molecules, they were placed initially near the two major grooves on the same side of DNA, and in the case of DNA−three dendrimers, two dendrimers were placed similarly in two major grooves on same side and the third dendrimer molecule was placed in the major groove on the opposite side and in between the two major grooves. The resulting complexes were put in a water box using the TIP3P water model.[62] To neutralize negative charges on the phosphate groups of DNA backbone, appropriate numbers of Na^+ ions were added. Also, Cl^- ions were added to neutralize the protonated primary amines on dendrimers. Minimization of solvated complexes was done in two steps. Steepest descent minimization, with 1000 steps, was followed by 2000 steps of conjugate gradient minimization. In order to remove bad contacts, starting conformation of the solute was kept fixed using harmonic constraint with a force constant of 500 kcal/mol/Å^2 with no constraints on ions and water. Minimized structure was then subjected to 40 ps of MD, using a 2 fs time step. During this period, using weak harmonic constraints of 20 kcal/mol/Å^2 on solute, system was gradually heated from 0 to 300 K. This allowed slow relaxation of solute. To prevent any dynamical changes in the NH and OH bonds from disrupting hydrogen bonds, SHAKE constraints using a geometrical tolerance of 5×10^{-4} Å were imposed on all covalent bonds involving hydrogen atoms.[63] Further constant pressure (NPT) MD was done with temperature regulation achieved using the Berendsen weak coupling method[64] (0.5 ps time constant for heat bath coupling and 0.2 ps pressure relaxation time). Again, conjugate gradient minimization of 5000 steps was carried with harmonic constraints decreasing from 20 kcal/mol/Å^2 to zero in steps of 5 kcal/mol/Å^2. This was followed by 100 ps unconstrained NPT MD to equilibrate system at 300 K. In our earlier work also we followed a similar protocol which provided stable and reliable MD results.[57,58] Finally, 20 to 50 ns long 300 K NVT MD runs were carried out using a heat bath coupling time constant of 1 ps. The electrostatic interactions were calculated with the particle mesh Ewald (PME) method.[64,65]

Atomic Force Microscopy. Dendrimer−pcDLucDNA complexes were prepared at ratios R of 1:1 and 5:1, at a final DNA concentration of 0.1 ng mL^{-1}. For each sample, 5 μL aliquot was adsorbed on mica-V1, followed by a wash with nuclease-free water to remove the unadsorbed sample, and dried under nitrogen stream. The samples were imaged using Veeco diInnova AFM (Bruker, USA) under tapping mode in air. The resonance frequency of tapping mode cantilever was set at 291 kHz and scanning rate was 0.5 Hz.

Zeta Potential Measurements. Aq solutions of pEGFP−dendrimer complexes at the required weight ratios (R) were made by mixing pEGFP (10 μg/mL) with the required amounts of dendrimer (stock solution 10 mg/mL) in HEPES Buffer (pH = 7.4) and equlibrating at room temperature for 20 min. The zeta potential and electrophoretic mobility measurements were carried out on Brookhaven ZetaPals instrument at a controlled temperature of 25 ± 0.5 °C. Each data is taken as an average of three runs with each run comprising ten measurements. The zeta potential of pEGFP (10 μg/mL) and dendrimer (50 μg/mL) were also measured.

Expression Vectors, Cells, and Media. The plasmids, pEGFP, and pcDNA Luc were amplified in competent *E. coli* DH5α cells and isolated using standard protocols. The purity of plasmids was checked by electrophoresis on a 0.8% agarose gel and the DNA was quantified by determining absorbance at 260 nm. Cell monolayers were maintained in Dulbecco's modified Eagle's medium (DMEM) supplemented with 10% heat-inactivated fetal bovine serum (FBS) and 1% penicillin−streptomycin at 37 °C in 5% CO_2.

Complexation Assay. Dendrimer−DNA complexes were prepared at ratios by coincubating at room temperature, defined amounts of PETIM dendrimer with 1 μg of the plasmid separately in PBS (pH∼7.4) in a total volume of 20 μL. After 20 min, the formation of complexes was assessed by gel retardation assay by running the complexes through 0.8% agarose gel using a Tris acetate-EDTA (pH ∼ 8) electrophoresis system. The DNA was visualized using ethidium bromide staining and were documented using a gel documentation system.

Cytotoxicity Assay. In a 96 well plate, 5×10^3 cells were seeded and allowed to grow for 16 h at 37 °C under 5% CO_2 conditions. The medium in the wells was then replaced with fresh medium, increasing concentrations of dendrimer added, and further, the plate was incubated for 24 h at 37 °C in the presence of 5% CO_2. 20 μL of MTT reagent (5 mg mL^{-1}) was then added in to the wells and kept for 4 h in the dark at 37 °C. The resultant formazone crystals were dissolved in 100 μL of DMSO, and the absorbance was recorded at 570 nm. Untreated cells were used as controls. The results represent an average of three such experiments in duplicate.

Transfection Protocol. One $\times 10^5$ cells were grown in a 12 well plate to 60% confluency at 37 °C in a humidified atmosphere containing 5% CO_2. Dendrimer−DNA complexes were prepared at various ratios (R) using plasmid (3 μg) and the required amount of dendrimer by incubating in Opti-MEM for 20 min. The cells were washed twice with PBS and were incubated with the complexes in Opti-MEM for 4 h. After the transfection time, the cells were incubated with complete growth medium, DMEM for up to 48 h. Live images of the transfected cells were captured with a fluorescent microscope (Leica) using a filter for 475 nm. For quantification of the transfection levels, the dendrimer−pcDNA Luc complexes were formed at a constant R of 15:3 (μg) and were transfected in a similar manner to that described above. At 24 and 48 h the cells were collected in 1X Passive Lysis Buffer (PLB). The cell lysate were then vortexed, spun at 3000 rpm for 15 min at 4 °C, and the supernatant was assayed for luminescence.

Luciferase Assay. Luciferase assay was performed using Dual luciferase assay kit and the activities were measured in the luminometer. The amount of protein was quantified using the standard Bradford assay and the readings were normalized to 1 μg of protein concentration. The experiments were done in triplicate and the data is represented as a standard error of mean.

■ ASSOCIATED CONTENT

Supporting Information

Details of synthesis and characterization of the dendrimer. This material is available free of charge via the Internet at http://pubs.acs.org.

■ AUTHOR INFORMATION

Corresponding Author

*E-mail: jayaraman@orgchem.iisc.ernet.in.

Notes

The authors declare no competing financial interest.

■ ACKNOWLEDGMENTS

We thank Department of Biotechnology (DBT), New Delhi, for financial support. A.L. and K.S.V. thank Council for Scientific and Industrial Research (CSIR), India, for a research fellowship.

■ REFERENCES

(1) Medina, S., and El-Sayed, M. E. H. (2009) Dendrimers as carriers for delivery of chemotherapeutic agents. *Chem. Rev. 109*, 3141−3157.

(2) Patri, A. K., and Simanek, E. (2012) Biological applications of dendrimers. *Mol. Pharmaceutics 9*, 341.

(3) Fernandez, C. A., and Rice, K. G. (2009) Engineered nanoscaled polyplex gene delivery systems. *Mol. Pharmaceutics 6*, 1277−1289.

(4) Duncan, R. (2003) The dawning era of polymer therapeutics. *Nat. Rev. Drug Discovery 2*, 347−360.

(5) Nori, A., and Kopeček, J. (2005) Intracellular targeting of polymer-bound drugs for cancer chemotherapy. *Adv. Drug Delivery Rev. 57*, 609−639.

(6) Srinivasachari, S., Fichter, K. M., and Reineke, T. M. (2008) Polycationic β-cyclodextrin "click clusters": Monodisperse and versatile scaffolds for nucleic acid delivery. *J. Am. Chem. Soc. 130*, 4618−4627.

(7) Kukowska-Latallo, J. F., Bielinska, A., Johnson, J., Splinder, R., Tomalia, D. A., and Baker, J. R. (1996) Efficient transfer of genetic material into mammalian cells using starburst polyamidoamine dendrimers. *Proc. Natl. Acad. Sci. U.S.A. 93*, 4897−4902.

(8) Hensler, J., and Szoka, F. C. (1993) Polyamidoamine cascade polymers mediate efficient transfection of cells in culture. *Bioconjugate Chem. 4*, 372−379.

(9) Maiti, P. K., and Bagchi, B. (2006) Structure and dynamics of DNA-dendrimer complexation: Role of counterions, water, and base pair sequence. *Nano Lett. 6*, 2478−2485.

(10) Nandy, B., and Maiti, P. K. (2011) DNA compaction by a dendrimer. *J. Phys. Chem. B 115*, 217−230.

(11) Tsai, Y.-J., Hu, C.-C., Chu, C.-C., and Imae, T. (2011) Intrinsically fluorescent PAMAM dendrimer as gene carrier and nanoprobe for nucleic acids delivery: Bioimaging and transfection study. *Biomacromolecules 12*, 4283−4290.

(12) Agrawal, A., Min, D.-H., Singh, N., Zhu, H., Birjiniuk, A., von Maltzahn, G., Harris, T. J., Xing, D., Woolfenden, S. D., Sharp, P. A., Charest, A., and Bhatia, S. (2009) Functional delivery of siRNA in mice using dendriworms. *ACS Nano 3*, 2495−2504.

(13) Luo, D., Haverstick, K., Belvheva, N., Han, E., and Saltzman, W. M. (2002) PAMAM-PEG-PAMAM: Novel triblock copolymer as a biocompatible and efficient gene delivery carrier. *Macromolecules 35*, 3456−3462.

(14) Kim, T. -I., Seo, H. J., Choi, J. S., Jang, H. -S., Baek, J. -U., Kim, K., and Park, J. -S. (2004) Poly(ethylene glycol)-conjugated PAMAM dendrimer for biocompatible, high-efficiency DNA delivery. *Biomacromolecules 5*, 2487−2492.

(15) Yuan, Q., Yeudall, W. A., and Yang, H. (2010) PEGylated polyamidoamine dendrimers with bis-aryl hydrazone linkages for enhanced gene delivery. *Biomacromolecules 11*, 1940−1947.

(16) Liu, H., Wang, H., Yang, W., and Cheng, Y. (2012) Disulfide cross-linked low generation dendrimers with high gene transfection efficacy, low cytotoxicity, and low cost. *J. Am. Chem. Soc. 134*, 17680−17687.

(17) Santos, J. L., Oliveira, H., Pandita, D., Rodigues, J., Pego, A. P., Granja, P. L., and Tomas, H. (2010) Functionalization of poly(amidoamine) dendrimers with hydrophobic chains for improved gene delivery in mesenchymal stem cells. *J. Controlled Release 144*, 55−64.

(18) Pandita, D., Santos, J. L., Rodigues, J., Pego, A. P., Granja, P. L., and Tomas, H. (2011) Gene delivery into mesenchymal stem cells: A biomimetic approach using RGD nanoclusters based on poly(amidoamine) dendrimer. *Biomacromolecules 12*, 472−481.

(19) Choi, J. S., Nam, K., Park, J. -Y., Kim, J. -B., Lee, J. -K., and Park, J. -S. (2004) Enhanced transfection efficiency of PAMAM dendrimer by surface modification with L-arginine. *J. Controlled Release 99*, 445−456.

(20) Wada, K., Arima, H., Tsutsumi, T., Chihara, Y., Hattori, K., Hirayama, F., and Uekama, K. (2005) Improvement of gene delivery mediated by mannosylated dendrimer/α-cyclodextrin conjugates. *J. Controlled Release 104*, 397−413.

(21) Wood, K. C., Azarin, S. M., Arap, W., Pasqualini, R., Langer, R., and Hammond, P. T. (2008) Tumor-targeted gene delivery using molecularly engineered hybrid polymers functionalized with a tumor-homing peptide. *Bioconjugate Chem. 19*, 403−405.

(22) Waite, C. L., and Roth, C. M. (2009) PAMAM-RGD conjugates enhance siRNA delivery through a multicellular spheroid model of malignant glioma. *Bioconjugate Chem. 20*, 1908−1916.

(23) Zhang, X. -Q., Wang, X. L., Huang, S. -W., Zhuo, R. -X., Liu, Z. -L., Mao, H. -Q., and Leong, K. W. (2005) *In vitro* gene delivery using polyamidoamine dendrimers with a trimesyl core. *Biomacromolecules 6*, 341−350.

(24) Zhou, J., Wu, J., Hafid, N., Behr, J. -P., Erbacher, P., and Peng, L. (2006) PAMAM dendrimers for efficient siRNA delivery and potent gene silencing. *Chem. Commun.*, 2362−2364.

(25) Liu, X., Liu, C., Laurini, E., Posocco, P., Pricl, S., Qu, F., Rocchi, P., and Peng, L. (2012) Polyamidoamine dendrimers with a modified pentaerythritol core having high efficiency and low cytotoxicity as gene carriers. *Mol. Pharmaceutics 9*, 470−481.

(26) Wang, Y., Kong, W., Song, Y., Duan, Y., Wang, L., Steinhoff, G., Kong, D., and Yaoting, Y. (2009) Polyamidoamine dendrimers with a modified pentaerythritol core having high efficiency and low cytotoxicity as gene carriers. *Biomacromolecules 10*, 617−622.

(27) Ghosh, P. S., Kim, C.-K., Han, G., Forbes, N. S., and Rotello, V. M. (2008) Efficient gene delivery vectors by tuning the surface charge density of amino acid-functionalized gold nanoparticles. *ACS Nano 2*, 2213−2218.

(28) Chen, A. M., Tarantula, O., Wei, D., Yen, H.-I., Thomas, T., Thomas, T. J., Minko, T., and He, H. (2010) Labile catalytic packaging of DNA/siRNA: Control of gold nanoparticles "out" of DNA/siRNA complexes. *ACS Nano 4*, 3679−3688.

(29) Rosenholm, J. M., Meinander, A., Peuhu, E., Niemi, N., Eriksson, J. E., Sahlgren, C., and Linden, C. (2009) Targeting of porous hybrid silica nanoparticles to cancer cells. *ACS Nano 3*, 197−206.

(30) Radu, D. R., Lai, C. -Y., Jeftinija, K., Rowe, E. W., Jeftinija, S., and Lin, V. S. -Y. (2004) A polyamidoamine dendrimer-capped mesoporous silica nanosphere-based gene transfection reagent. *J. Am. Chem. Soc. 126*, 13216−13217.

(31) Mintze, A. M., and Simanek, E. E. (2009) Nonviral vectors for gene delivery. *Chem. Rev. 109*, 259−302.

(32) Thankappan, U. P., Madhusudana, S. M., Desai, A., Jayamuragan, G., Rajesh, Y. B. R. D., and Jayaraman, N. (2011) Dendritic poly(ether imine) based gene delivery vector. *Bioconjugate Chem. 22*, 115−119.

(33) Krishna, T. R., and Jayaraman, N. (2003) Synthesis of poly(propyl ether imine) dendrimers and evaluation of their cytotoxic properties. *J. Org. Chem. 68*, 9694−9704.

(34) Cantor, C. R., and Schimmel, P. R. (1980) Hypochromism in chromophore aggregates, in *Biophysical Chemistry Part II. Techniques*

for the study of biological structure and function, pp 399−404, Chapter 7, W. H. Freeman and Company, New York.
(35) Ottaviani, M. F., Furini, F., Casini, A., Turro, N. J., Jockusch, S., Tomalia, D. A., and Messori, L. (2000) Formation of supramolecular structures between DNA and starburst dendrimers studied by EPR, CD, UV and melting profiles. *Macromolecules 33*, 7842−7851.
(36) Rodiguez-Pulido, A., Ortega, F., Llorca, O., Aicart, E., and Junquera, E. A. (2008) Physicochemical characterization of the interaction between DC-Chol/DOPE cationic liposomes and DNA. *J. Phys. Chem. B 112*, 12555−12565.
(37) Case, D. A., Darden, T. A., Cheatham, T. E., Simmerling, C. L., Wang, J., Duke, R. E., Luo, R., Walker, R. C., Zhang, W., Merz, K. M., Roberts, B., Wang, B., Hayik, S., Roitberg, A., Seabra, G., Kolossváry, I., Wong, K. F., Paesani, F., Vanicek, J., Liu, J., Wu, X., Brozell, S. R., Steinbrecher, T., Gohlke, H., Cai, Q., Ye, X., Wang, J., Hsieh, M. J., Cui, G., Roe, D. R., Mathews, D. H., Seetin, M. G., Sagui, C., Babin, V., Luchko, T., Gusarov, S., Kovalenko, A., and Kollman, P. A. *AMBER 11*; University of California, San Francisco, 2010.
(38) Volcke, C., Pirotton, S., Grandfils, C., Humbert, C., Thiry, P. A., Ydens, I., Dubois, P., and Raes, M. (2006) Influence of DNA condensation state on transfection efficiency in DNA/polymer complexes: An AFM and DLS comparative study. *J. Biotechnol. 125*, 11−21.
(39) Storkle, D., Duschner, S., Heimann, N., Maskos, M., and Schmidt, M. (2007) Complex formation of DNA with oppositely charged polyelectrolytes of different chain topology: Cylindrical brushes and dendrimers. *Macromolecules 40*, 7998−8006.
(40) Schmatko, T., Muller, P., and Maaloum, M. (2012) Surface charges effects on the 2D conformation of supercoiled DNA. *arXiv:1205* 2991v1.
(41) Bezanilla, M., Manne, S., Laney, D.-E., Yuri, L., Lyubchenko, G., and Hansma, H. G. (1995) Adsorption of DNA to mica, silylated mica, and minerals: Characterization by atomic force microscopy. *Langmuir 11*, 655−659.
(42) Ritort, F., Mihardja, S., Smith, S. B., and Bustamante, C. (2006) Condensation transition in DNA-polyaminoamide dendrimer fibers studied using optical tweezers. *Phys. Rev. Lett. 96*, 118301−118304.
(43) Fant, K., Esbjörner, E. K., Lincoln, P., and Norden, B. (2008) DNA condensation by PAMAM dendrimers: Self-assembly characteristics and effect on transcription. *Biochemistry 47*, 1732−1740.
(44) Froehlich, E., Mandeville, J. S., Weinert, C. M., Kreplak, L., and Tajmir-Riahi, H. A. (2011) Bundling and aggregation of DNA by cationic dendrimers. *Biomacromolecules 12*, 511−517.
(45) Malik, N., Wiwattanapatapee, R., Klopsch, R., Lorenz, K., Frey, H., Weener, J. W., Meijer, E. W., Paulus, W., and Duncan, R. (2000) Dendrimers: Relationship between structure and biocompatibility in vitro, and preliminary studies on the biodistribution of ^{125}I-labelled polyamidoamine dendrimers *in vivo*. *J. Controlled Release 65*, 133−148.
(46) Duncan, R., and Izzo, L. (2005) Dendrimer biocompatibility and toxicity. *Adv. Drug Delivery Rev. 57*, 2215−2237.
(47) Chonco, L., Bermejo-Martín, J. F., Ortega, P., Shcharbin, D., Pedziwiatr, E., Klajnert, B., de la Mata, F. J., Eritja, R., Gómez, R., Bryszewska, M., and Muñoz-Fernandez, M. A. (2007) Water-soluble carbosilane dendrimers protect phosphorothioate oligonucleotides from binding to serum protein. *Org. Biomol. Chem. 5*, 1886−1893.
(48) Padié, C., Maszewska, M., Majchrzak, K., Nawrot, B., Caminade, A.-M., and Majoral, J.-P. (2009) Polycationic phosphorus dendrimers: synthesis, characterization, study of cytotoxicity, complexation of DNA, and transfection experiments. *New J. Chem. 33*, 318−326.
(49) Wasiak, T., Ionov, M., Nieznanski, K., Nieznanska, H., Klementieva, O., Granell, M., Cladera, J., Majoral, J. P., Caminade, A.-M., and Klajnert, B. (2012) Phosphorus dendrimers affect alzheimer's ($A\beta_{1-28}$) peptide and MAP-Tau protein aggregation. *Mol. Pharmaceutics 9*, 458−489.
(50) Kafil, V., and Omidi, Y. (2011) Cytotoxic impacts of linear and branched polyethylenimine nanostructures in A431 cells. *BioImpacts 1*, 23−30.
(51) Tang, R., Ji, W., and Wang, C. (2011) Synthesis and characterization of new poly(ortho ester amidine) copolymers for non-viral gene delivery. *Polymer 52*, 921−932.
(52) Breunig, M., Lungwitz, U., Liebl, R., and Goepferich, A. (2007) Breaking up the correlation between efficacy and toxicity for nonviral gene delivery. *Proc. Natl. Acad. Sci. U.S.A. 104*, 14454−14459.
(53) Bielinska, A. U., Kukowska-Latallo, J. F., and Baker, J. R. (1997) The interaction of plasmid DNA with polyamidoamine dendrimers: mechanism of complex formation and analysis of alterations induced in nuclease sensitivity and transcriptional activity of the complexed DNA. *Biochim. Biophys. Acta 1353*, 180−190.
(54) Pack, D. W., Hoffman, A. S., Pun, S., and Stayton, P. S. (2005) Design and development of polymers for gene delivery. *Nat. Rev. Drug Discovery 4*, 518−593.
(55) Baker, A., Saltik, M., Lehrmann, H., Killisch, I., Mautner, V., Lamm, G., Christofori, G., and Cotton, M. (1997) Polyethylenimine (PEI) is a simple, inexpensive and effective reagent for condensing and linking plasmid DNA to adenovirus for gene delivery. *Gene Ther. 4*, 773−782.
(56) Maingi, V., Jain, V., Bharatam, P. V., and Maiti, P. K. (2012) Dendrimer building toolkit: Model building and characterization of various dendrimer architectures. *J. Comput. Chem. 33*, 1997−2011.
(57) Maiti, P. K., Pascal, T. A., Vaidehi, N., and Goddard, W. A. (2004) The stability of Seeman JX DNA topoisomers of paranemic crossover (PX) molecules as a function of crossover number. *Nucleic Acids Res. 32*, 6047−6056.
(58) Maiti, P. K., Pascal, T. A., Vaidehi, N., Heo, J., and Goddard, W. A. (2006) Atomic-level simulations of Seeman DNA nanostructures: The paranemic crossover in salt solution. *Biophys. J. 90*, 1463−1479.
(59) Cornell, W. D., Cieplak, P., Bayly, C. I., Gould, I. R., Merz, K. M., Ferguson, D. M., Spellmeyer, D. C., Fox, T., Caldwell, J. W., and Kollman, P. A. (1996) A second generation force field for the simulation of proteins, nucleic acids, and organic molecules. *J. Am. Chem. Soc. 118*, 2309−2309.
(60) http://www.physics.iisc.ernet.in/~maiti/dbt/home.html.
(61) Wang, J., Wolf, R. M., Caldwell, J. W., Kollman, P. A., and Case, D. A. (2004) Development and testing of a general amber force field. *J. Comput. Chem. 25*, 1157−1174.
(62) Jorgensen, W. L., Chandrasekhar, J., Madura, J. D., Impey, R. W., and Klein, M. L. (1983) Comparison of simple potential functions for simulating liquid water. *J. Chem. Phys. 79*, 926−935.
(63) Ryckaert, J. -P., Ciccotti, G., and Berendsen, H. J. C. (1977) Numerical integration of the cartesian equations of motion of a system with constraints: molecular dynamics of *n*-alkanes. *J. Comput. Phys. 23*, 327−341.
(64) Berendsen, H. J. C., Postma, J. P. M., van Gunsteren, W. F., DiNola, A., and Haak, J. R. (1984) Molecular dynamics with coupling to an external bath. *J. Chem. Phys. 81*, 3684−3690.
(65) Darden, T., York, D., and Pedersen, L. (1993) Particle mesh Ewald: An $N\cdot\log(N)$ method for Ewald sums in large systems. *J. Chem. Phys. 98*, 10089−11092.
(66) Vasumathi, V., and Maiti, P. K. (2010) Complexation of siRNA with dendrimer: A molecular modeling approach. *Macromolecules 43*, 8264−8274.